Available online at www.sciencedirect.com
SCIENCE DIRECT®
Earth and Planetary Science Letters 244 (2006) 1 – 15
EPSL
www.elsevier.com/locate/epsl

1300-m-high rising bubbles from mud volcanoes at 2080 m in the Black Sea: Hydroacoustic characteristics and temporal variability

Jens Greinert [a,*], Yuriy Artemov [b], Viktor Egorov [b], Marc De Batist [c], Daniel McGinnis [d]

[a] *Leibniz-Institute of Marine Sciences at Kiel University (IFM-GEOMAR), Wischhofstrasse 1-3, D-24148 Kiel, Germany*
[b] *Institute of Biology of the Southern Seas (IBSS), Nakhimov Prosp., UA-99011 Sevastopol, Ukraine*
[c] *Renard Centre of Marine Geology at Ghent University (RCMG), Krijgslaan 281 s.8, B-9000 Gent, Belgium*
[d] *Swiss Federal Institute for Environmental Science and Technology (EAWAG), Seestrasse 79, CH-6047 Kastanienbaum, Switzerland*

Received 23 September 2005; received in revised form 30 January 2006; accepted 2 February 2006

Editor: H. Elderfield

Abstract

A mud volcano area in the deep waters (>2000 m) of the Black Sea was studied by hydroacoustic measurements during several cruises between January 2002 and June 2004. Gas bubbles in the water column give strong backscatter signals and thus can be detected even in great water depths by echosounders as the 38 kHz EK500 scientific split-beam system that was used during the surveys. Because of their shape in echograms and to differentiate against geochemical plumes and real upwelling bubble-water plumes, we call these hydroacoustic manifestations of bubbles in the water column 'flares'. Digital recording and processing of the data allows a 3D visualization and data comparison over the entire observation period, without artefacts caused by changing system settings.

During our surveys, we discovered bubble release from three separate mud volcanoes, Dvurechenskiy (DMV), Vodianitskiy (VMV) and the Nameless Seep Site (NSS), in about 2080 m water depth simultaneously. Bubble release was observed between 9 June 2003 and 5 June 2004. The most frequently surveyed, DMV, was found to be inactive during very intensive studies in January 2002. The first activity was observed on 27 June 2002, which finally ceased between 5 and 15 June 2004 after a period of continuously decreasing activity. This observed 2-yr bubble-release period at a mud volcano may give an indication for the duration of active periods. The absence of short-term variations (within days or hours) may indicate that the bubble release from the observed mud volcanoes does not undergo rapid changes. The recorded echograms show that bubbles rise about 1300 m high through the water column, to a final water depth of about 770 m, which is ~75 m below the phase boundary of pure methane hydrate in the Black Sea. With a release depth from 2068 m and a detected rise height of 1300 m, the flare at VMV is among the deepest and highest reported so far, and gives evidence of highly extended bubble life times (up to 108 min) in deep marine environments.

To better understand how a methane bubble (gas analyses of the pore water and gas hydrate gave 99.4% methane) can rise so high without dissolving, we applied a recently developed bubble dissolution model that takes into account a decreased mass transfer due to an immediately formed gas-hydrate rim. Using the hydroacoustically determined bubble rising speeds (19–22 cm/s at the bottom; 12–14 cm/s at the flare top) and the relation between the rising speed of 'dirty'/gas hydrate rimmed bubbles and the bubble size, we could validate that a gas-hydrate-rimmed bubble with a diameter of 9 mm could survive the 1300-m-rise through the water column, before it is finally dissolved. A diameter of about 9 mm is reasonable for bubbles released at seep sites and the

* Corresponding author. Current address: GNS Sciences, 1 Fairway Drive, Lower Hutt, New Zealand.
E-mail addresses: jgreinert@ifm-geomar.de, j.greinert@gns.cri.nz (J. Greinert).

0012-821X/$ - see front matter
doi:10.1016/j.epsl.2006.02.011

coincidence between the observed bubble rising speed and the model approach of a 9-mm bubble supports the assumption of gas-hydrate-rimmed bubbles.

Keywords: Sorokin Trough; Black Sea; mud volcanoes; bubble seepage; timely variability; hydroacoustic plume – flare; bubble dissolution modeling

1. Introduction

Methane seeps are currently a topic of strong interest in both marine and lacustrine research, particularly those seeps that are related to gas hydrate occurrences [1–7]. Methane fluxes at those seeps have a significant impact on the local and possibly regional carbon budgets and trigger the massive precipitation of carbonates (e.g. [8–10]). Microbial studies have shown that the anaerobic oxidation of dissolved methane (AOM) by a consortium of archaea and bacteria in the shallow sea-floor sediments [11–15] has an immense methane-filtering capability [16]. In contrast, the released free-gas phase is much less (if at all) directly influenced/consumed by microorganisms and is thus capable of transporting significant amounts of methane gas very rapidly into and through the water column. The fate of dissolved methane in the marine environment due to aerobic consumption [17], distribution [18] or formation in micro-environments at the base of the euphotic zone [19] are well understood. However, real data about the processes controlling gas bubbles, their lifetime, the gas

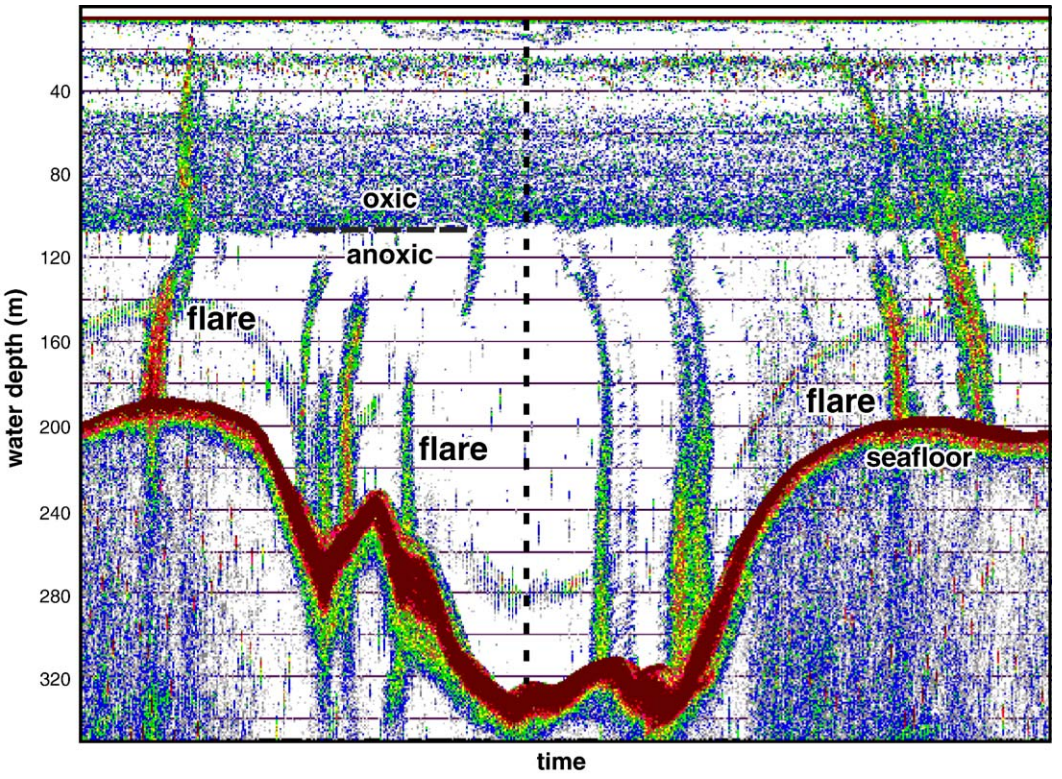

Fig. 1. Single-beam echogram showing a typical hydroacoustic manifestation of rising methane bubbles in flare-like shape in the Black Sea. The image shows several flares rising from different depths between 190 and 325 m (*x*-axis span ≈ 22 min), with shallower flares almost reaching the sea surface and crossing the oxic/anoxic boundary at about 110 m. The strong signals in the oxic zone above 110 m are caused by fish and zooplankton, whereas below this depth the Black Sea provides ideal conditions for detailed hydroacoustic studies of bubbles without other 'disturbing' backscattering. Flares are often tilted or bended because of currents. The bending of the flares towards the middle of the image is caused by the turn of the ship on an opposing course (dashed vertical line).

exchanges occurring between the bubble and the surrounding water or the formation of a gas-hydrate skin on the bubble surface are limited. This is to a large extent due to the technical difficulties of acquiring such data, which requires very sophisticated and expensive sampling procedures and tools (submersibles, ROVs) and is hampered by both the very small size of the bubble site itself and the temporal variability of the bubble release on very different time scales.

Nevertheless, many bubbling (i.e. free-gas releasing) cold seeps and hydrothermal vents are known from all over the world. These features are typically identified by hydroacoustic 'plumes' in the water column (i.e. strong backscatter signals with a flare-like shape that are detected with single-beam echosounders), which are often 'rooted' to the seafloor [1,20–29, and articles in 30]. Thus, echosounder systems of different kind have become a common tool for finding and monitoring bubbling seep sites. Use of sophisticated multi-frequency, split-beam systems allows detailed investigations of the bubble-size distribution, rising speeds and finally gas fluxes if the data are stored digitally [31]. The great advantage of hydroacoustics is that the bubble-releasing system itself – i.e. the seafloor with small fluid/gas pathways or currents in the bottom boundary layer – is not disturbed by this remote, non-invasive method.

Within the EU-funded project CRIMEA we studied a series of bubble-releasing seeps in the Black Sea to investigate the possible impact of 'high intensity seeps' on the atmospheric methane concentrations. Sites from 60 to 2100 m were hydroacoustically mapped and extensively sampled during several cruises between 2002 and 2004. Here, we report about the occurrence and temporal variability of three bubble-seep locations in more than 2000 m water depth (mwd) which generate more than 1000-m-high 'hydroacoustic plumes'.

In the following we will call these hydroacoustic plumes 'flares' because of their shape on echograms (Fig. 1) and to clearly distinguish between geochemical anomalies in the water column and those sites that imply the upward migration of water due to thermal heating (at hydrothermal vents/mud mounds) or massive bubble release [28,32], which are also called plumes.

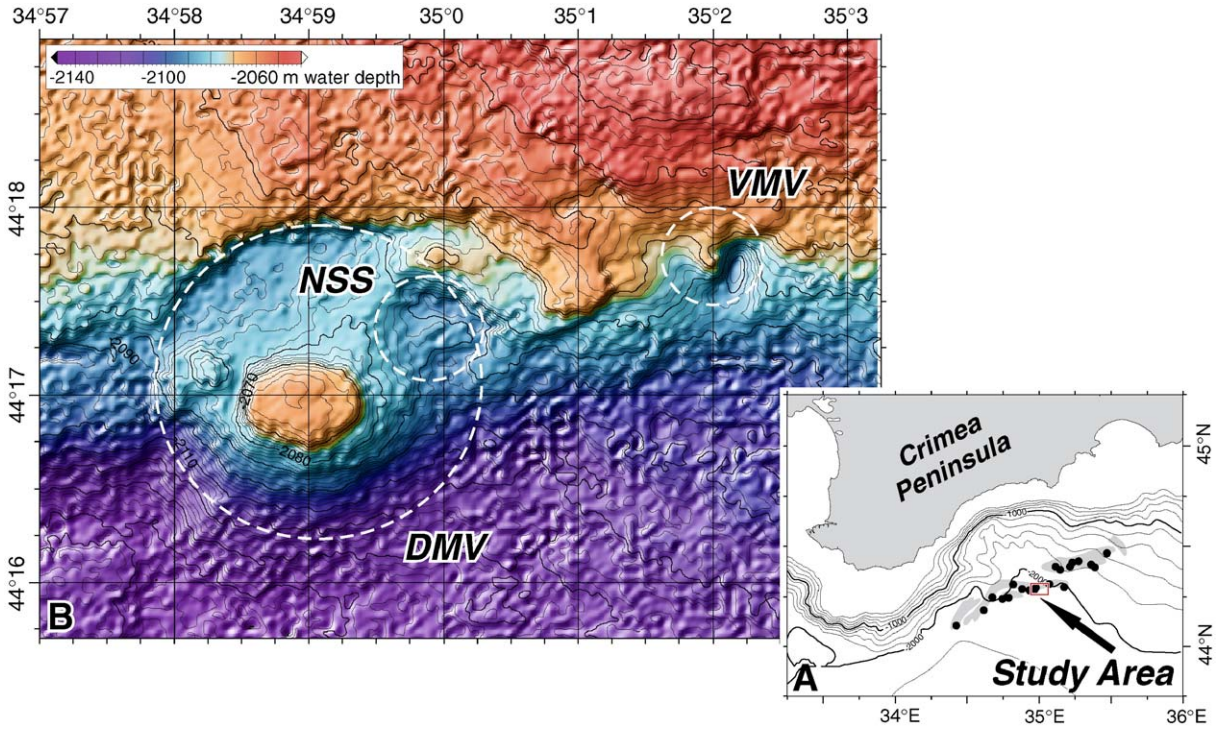

Fig. 2. (A) Position of the study area in the Black Sea, SE of the Crimea Peninsula (Ukraine). Little black dots indicate mud volcanoes, gray patches show the distribution of diapiric zones/faults (after Krastel et al. [34]). The sediments extruded from the mud volcanoes are clay-rich deposits from the Maikopian Formation that forms an Oligocene–Lower Miocene sequence of 4–5 km thickness [33]. (B) Bathymetric map of the study area with the locations of the investigated mud volcanoes Dvurechenskiy and Vodianitskiy (DMV, VMV) and the Nameless Seep Site (NSS). The overall depth range is from 2040 to 2140 m; the contour lines are in 2-m intervals with every 10-m annotate.

2. Study area

The flare sites are located in the Sorokin Trough, southeast of the Crimea Peninsula (Fig. 2). The Sorokin Trough is known for mud volcanoes of different size and shape in water depths between 1500 and 2100 m, fluid migration and gas hydrates occurrence [33–35]. Rather prominent is the Dvurechenskiy mud volcano (DMV), which, unlike most of the other mud volcanoes, has a very flat-topped central high [34] of 1.3 by 0.95 km situated in a larger caldera-like depression of 3.2 km in diameter (Fig. 2). The steep northern and western flank of this central 'mud pie' only rise 18 m above the depression bottom, whereas the eastern and southern flank decent from the top of the mud volcano at 2062 mwd down to 2130 mwd. Only 1.45 km NE and thus still within the main caldera, another small depression of 1.2 km in diameter occurs, showing a very weak central elevation (2089 m water depth) which we call the 'Nameless Seep Site' (NSS). Almost in the same direction as the NSS but 4.3 km away from DMV, a 20-m-deep depression builds the eastern flank of a third edifice, the Vodyanitskiy mud volcano (VMV), which is ~1 km in diameter. The VMV is morphologically part of the northward rising slope but builds a small brow at 2068 mwd.

Heat-flow measurements at DMV during cruises in May to June 2003 and 2004 confirm the data of Bohrmann et al. [33] and show constantly elevated values between DMV and VMV. Sediment sampling at DMV revealed cm-sized flake-shaped pieces of gas hydrate similar to previously sampled gas hydrate in the area. Immediate gas analyses of the sediment show methane as the main gas phase and traces of ethane (0.06% to 0.2%) and even smaller amounts of propane (Beaubien, personal communication). Similar gas compositions were analyzed by Blinova et al. [36] and were also found in pore-water data from mud volcanoes in the vicinity [37].

With respect to methane, the Black Sea is unique as the water column is characterized by a strong stratification in the upper 140–200 m where it changes from an oxic to anoxic environment [38–40]. The physical and geochemical conditions in the water column below 500 mwd of interest here show a steadily increasing temperature from 8.88 to 9.11 °C, a slight salinity increase and a σ_τ density profile which indicates almost complete mixing below 1800 mwd (Fig. 3). No dissolved oxygen exists below 500 mwd,

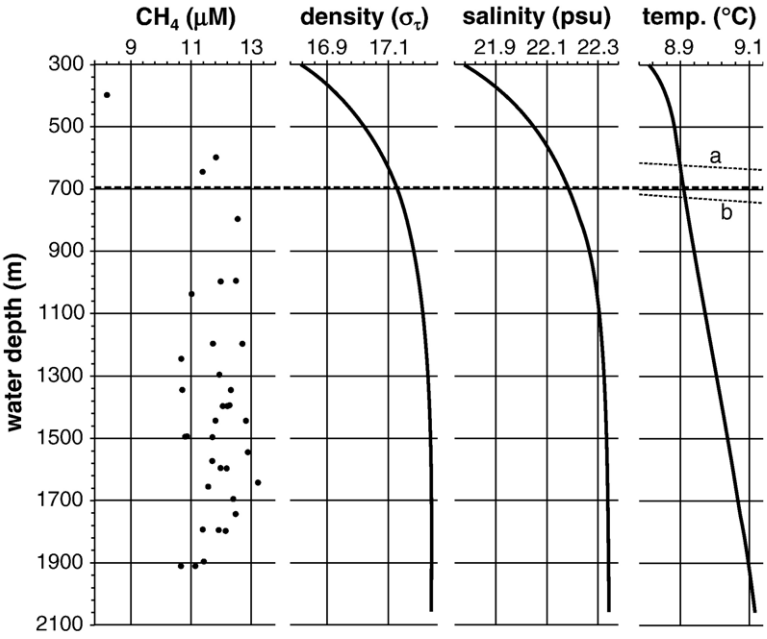

Fig. 3. CTD data and methane concentration form the study area. The density, salinity and temperature profiles are averaged from 12 individual casts which did not show significant differences with respect to the given scale. Methane concentrations are in the typical range for the anoxic water body of the Black Sea. The dashed line marks the phase boundary for pure methane hydrate at the ambient temperature and salinity conditions. Line a: phase boundary for methane hydrate in fresh water as calculated with CSMHYD. Line b: data from Dickens and Quinby-Hunt [48] for salt water with 33.5‰ salinity.

H_2S concentrations are in the range of 0.35 mM [35] and methane concentrations vary between 11 and 13 μM (Fig. 3). The latter is in good agreement with data presented by Reeburgh et al. [38]. The scattering in our methane data cannot be directly linked with sample distances to mud volcanoes or flares. Despite several attempts, we did not discover significantly higher methane concentrations above a mud volcano or within the hydroacoustic flare than we measured in their vicinity or at reference stations several kilometers away. A possible explanation for this is given by Schubert et al. [41] who argue that the methane input from bubbles is not high enough to cause a significant and detectable increase of the already very high dissolved methane concentration. N_2- and Ar-concentrations from the degassed water show concentrations between 600 and 690 μM (mean = 640 μM) and between 15 and 18 μM (mean = 16.5 μM), respectively.

Of great importance for the methane distribution and bubble release are currents and tides. Currents in the Black Sea are found to be rather weak below 500 mwd. ADCP measurements, visual observations in the water column and at the seafloor, as well as unpublished data (Korotaev, personal communication), give maximal current velocities in the range of 3 to 4 cm/s. Tides are almost absent in the Black Sea and daily water level changes vary in a range of 10–30 cm. Long-term variations in water level have been found to correlate with the North-Atlantic Oscillation, but even those changes are below 40 cm [42]. Thus, the influence of tides or currents on the release of bubbles should be negligible in more than 500 mwd.

3. Methods

For hydroacoustic investigations in 2003 and 2004 the dual-frequency scientific SIMRAD EK500 split-beam echosounder (38 and 120 kHz) on board *RV Professor Vodyanitskiy* was used. Due to the strong attenuation of high-frequency sound in water, all data shown here are only from the 38 kHz signal source. The beam angle of the system as defined by the −3 dB echo level is 6.7° which results in a footprint-to-depth ratio of about 1 : 8.5. The ping interval was 4.5 s with 3 ms pulse length. Hydroacoustic surveys were carried out at 4 to 5 knots, a speed at which the vessel steams rather silently. With 4.5-s ping interval, this results in a distance between two pings of about 10.5 m. More detailed measurements were done on drift, during which the main engine was switched off providing ideal conditions for hydroacoustic measurements. The system was calibrated during the cruises with a 30 mm reference target according to the method described by Anon [43].

When performing sequential hydroacoustic surveys or 'flare imaging', it is important to know exactly the specific system settings and to keep track of their variations during the survey (e.g. TVG, amplifications, filter, signal thresholds). Simple paper records or PC screen shots are therefore not adequate to provide quantitative scientific evidence of e.g. the flare height or changing bubble release intensities. All our data have been continuously recorded digitally including system settings and were post-processed with the WaveLens software (for detailed description of the used hydroacoustic techniques, see Artemov [31]). Typical echograms are shown in Fig. 4.

For the survey in January 2002, the Parasound system on board of *RV Meteor* was used which operates with 18 kHz as the main frequency of the parametric 3.5 kHz sub-bottom profiler unit (beam angle 4°). Unfortunately we were not able to calibrate the system during the cruise and thus are not totally sure about its accuracy. Nevertheless, during the same M52-1 cruise, the system proved its capability of detecting bubbles in the water column by recording several flares between 770 and 310 mwd further east of DMV [44]. As these detections occurred at shallower depth than the flare observations in the Sorokin Trough we compared the theoretical backscattering strength of bubbles smaller than 10 mm in diameter at 2000 mwd for 38 and 18 kHz. It is shown that the received signal strengths from 18 kHz would be significantly lower than the 38 kHz values for bubbles smaller than 4.4 mm in diameter (Fig. 5). For bubbles above 4.4 mm, the received 18 kHz signals would be generally stronger. These theoretical calculations concern methane bubbles without a hydrate skin, which if present may alter the acoustic properties of bubble. However, direct confirmation of hydrate-coated gas bubbles above DMV has not been obtained yet.

Water-column measurements and water sampling were performed with a SeaBird 911-plus CTD with water-sampling carrousel. CTD data were processed with the SeaBird post processing software. Measurements of the dissolved gases occurred directly on board using a vacuum degassing line [45,46] and GC-based gas analyses.

The phase boundary of the gas-hydrate stability zone (GHSZ) was calculated for the ambient pressure, temperature and salinity conditions. The CSMHYD program by Sloan [47] was used and a salinity correction based on Dickens and Quinby-Hunt [48] (here: 22.2‰ salinity = −0.73 °C) was applied, resulting

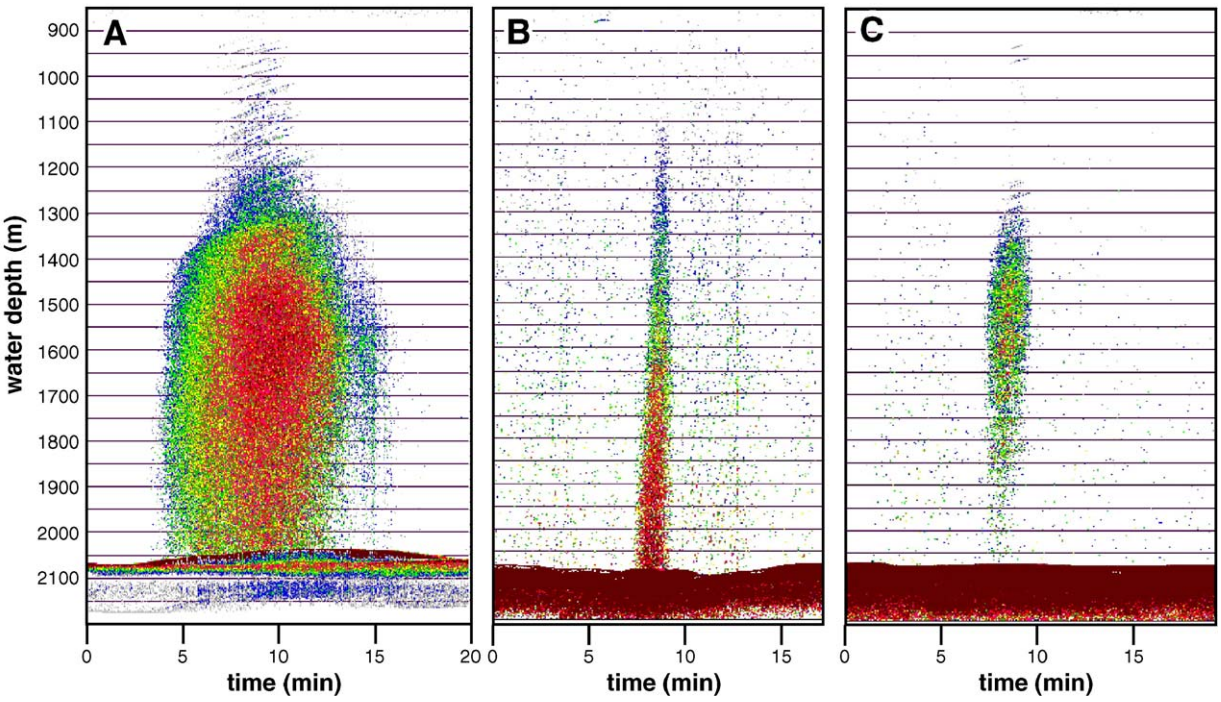

Fig. 4. Typical echograms recorded in the study area at different times and locations. (A) Date from VMV recorded at the 10 June 2003. The good data quality is due to very calm sea conditions at time of recording and because the ship was on drift with switched off main engine. (B) Date recorded from NSS at the 25 June 2003. The much thinner flare compared to image A is given due to the ships' speed of about 5 knots, which cased the higher noise. (C) Date from DMV recorded at the 2 June 2004, the last time bubbles where recorded above DMV. Images B and C are from Egorov et al. [61].

in a phase boundary for pure methane hydrate in the Black Sea at 695 mwd (Fig. 3). Suggesting that 0.1% of the gas phase is ethane, the phase boundary would be in about 690 mwd.

Bubble model calculations are based on the approach presented by McGinnis et al. [49], which incorporates the non-ideal gas equation and considers the salinity and pressure effects (fugacity) on gas solubility, and is suitable for a wide range of aquatic environments. The model tracks an individual bubble rising through the water column and calculates the gas exchange (i.e. stripping and dissolution) for four different gasses simultaneously (CO_2, CH_4, N_2 and O_2). The modelled bubble changes diameter due to the gas exchange, pressure, and temperature changes. Predicting the correct initial bubble size is critical as both the bubble rise velocity and mass transfer coefficient are bubble-size dependent. The model also predicts the rate of gas exchange for a bubble that has formed a methane-hydrate skin. Methane-hydrate skins form on bubbles

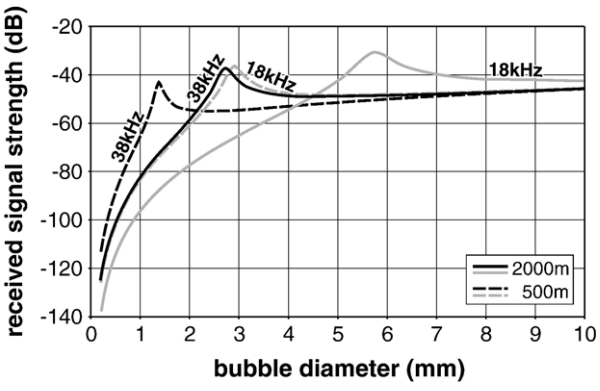

Fig. 5. Differences in the received signal strength of 18 and 38 kHz in 2000 and 500 m water depth for an ideal round gas bubble of different sizes.

released below the GHSZ, as reported by Rehder et al. [50] and dramatically extend the lifetime of the bubble, resulting in a substantially higher bubble rise height. The model by McGinnis et al. [49] has been calibrated to fit data by Rehder et al. [50] collected below and above the GHSZ.

4. Results and discussion

4.1. Flare observations and their temporal variability

Bubble release from DMV was first discovered 27 June 2002 using the EK500 during a short mapping survey as part of the PV57 cruise of *RV Professor Vodyanitskiy* [51,52]. Only 6 months earlier, DMV had been the target of very intensive investigations (pore water and water-column studies, sea-floor imaging and hydroacoustics) during the *RV Meteor* M52-1 cruise [33–36]. No bubbles were detected at that time using the 18 kHz Parasound system. With respect to the backscattering strength calculations shown in Fig. 5, the not-detection of bubbles above DMV in January 2002 indicates that (1) no bubbles larger than 4.4 mm were present, as those would have been easily detected; (2) that only some bubbles smaller than 4.4 mm might have been present but could not been detected because of the relatively low received target strength; or (3) that no bubbles at all were in the water column. In any case, it can be stated decisively that the amount of bubbles above DMV was significantly lower in January 2002

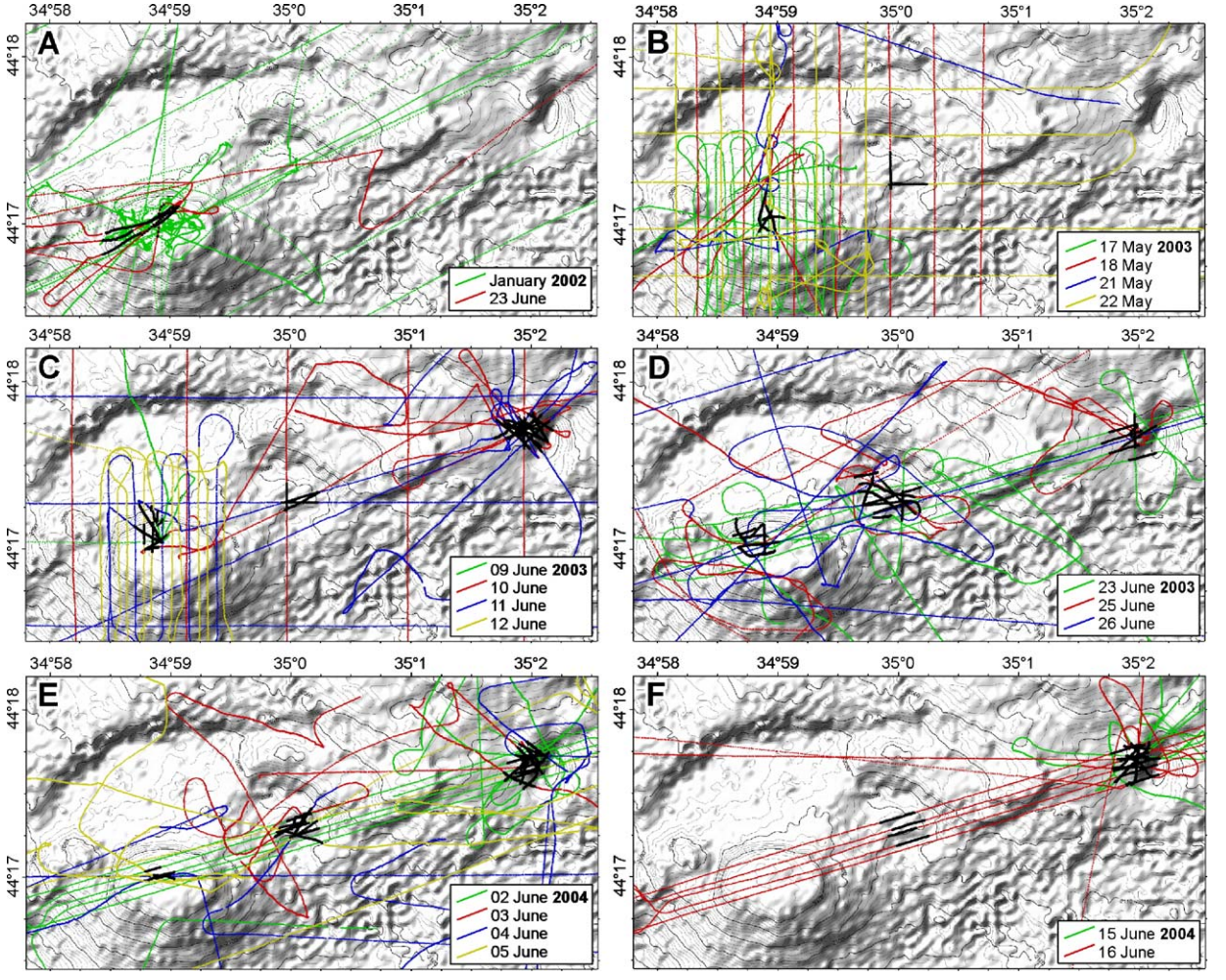

Fig. 6. (A–F) Tracks and flare occurrences during the 2002, 2003 and 2004 cruises. The green line in the 2002 map represents the track of cruise M52-1 with *RV Meteor* using the 18 kHz signal of the Parasound system. All other observations were done with the EK500 on board of *RV Professor Vodyanitskiy*. Black lines represent the positions projected on the seafloor where strong backscattering of bubbles–flares–have been observed. These observations are not corrected for the footprint and thus give a larger area than the actual bubble occurrence is.

than 6 months later during the first discovery of bubble release in the study area.

In June 2002, four lines in NE–SW direction detected two separate flares, one on top and one at the SW edge of the central high at DMV. With respect to other flares, both show a rather broad base of about 400 m width and a height of 710 and 740 m, respectively (Fig. 6A). One N–S running line crossing the eastern flare shows the same rise height as the central NE–SW running line, strongly supporting that the top of this flare is at 1320 mwd, with a total height of 740 m. Because of the similar readings on both crossing lines and the very symmetrical shape of the flare we are convinced that we crossed the flare at it highest point and that the observed rising height of 740 m represents the limit at which an unknown (few) amount of bubbles are still just detectable with the used system.

We do realize that statements of maximum rising heights of flares have to be made with caution, while taking into account the 3-dimensional hydroacoustic coverage of the flare and the type of hydroacoustic system (frequency and beam angle) that was used. This is of particular importance if relations between the rising height and e.g. methane anomalies in the water or the gas-hydrate phase boundary are discussed [29]. Nevertheless, if a flare is crossed from several different directions in a rather short time period (which depends on the assumed/known changes in the activity of the seep, the water depth and beam width) the detected maximum rising height can be taken as correct. Discussions about very-short-term changes of the activity-driven rise height or influences of currents that might move the top of the flare out of the beam during each crossing are, at a certain stage, irrelevant if the same rising height is found more than once within a reasonably short time.

It can be argued by the three crossings of the western flare that we did not hit the point of the maximum rising height, as the flares become higher from the southernmost line, from 560 m over 700 m to 740 m at the northernmost line. This may indicate that the highest point of the flare is further to the north (Figs. 6A and 7A).

The Gaussian shape of these two flares strongly indicates that no strong currents exist. Currents would change the 3-dimensional shape of a flare by adding a horizontal component to the almost straight upward migration of bubbles, which would result in tilted or bent flares as shown in Fig. 1. Current-driven shifting of bubbles is described by e.g. Merewether et al. [20] and shown in many published echograms. During our studies, it was commonly observed at shallower-water depths where currents of more than 40 cm/s were present. For a 740-m-high flare and the slowest observed bubble rising speed of 12 cm/s (see below) the maximal horizontal offset caused by a constant current of 3.5 cm/s would be 215 m. Thus, tilting or bending of flares would be well visible in 3-dimensionally visualized flares as it would be in normal echograms. However, significantly tilted or bended flares have never been observed in the Sorokin Trough area, and only the last observations of bubbles above DMV showed a flare that was not connected with the seafloor.

Based on the observation of bubble release at DMV in 2002, the area was surveyed again in May and June 2003, in the framework of the CRIMEA project (i.e. for multi-channel seismic studies, multi-beam mapping and parallel-running hydroacoustic single-beam surveys). A rather dense track grid, with a spacing of only 100 m, crossed DMV many times on 17 May 2003. Wider-spaced grids were sailed on 18 and 22 May 2003. All crossings show that only one flare is present at DMV, which is slightly shifted to the north from the middle of the flat-topped central high (Fig. 6B) indicating that the actual bubble releasing site has moved over the time. In addition, we localized a second flare at NSS for the first time on two lines. The flare height at DMV of 837 m (top at 1223 mwd) was slightly higher than at NSS, which in contrast showed much stronger volume backscattering strength of up to −50 dB (Fig. 7B). Unfortunately, we did not cross the area of VMV and thus have no information about the presence of bubbles for this time period at this mud volcano.

The flares of DMV and NSS were observed again during a return survey from 9 to 12 June 2003. In addition, we discovered bubble activity at VMV and due to its strong backscatter intensity and flare height (−48 dB and 1300 m, respectively), detailed CDT profiling and water sampling were undertaken to identify (a) bubble- or heat-influenced turbulence in the water column (evidence of a plume?), (b) the impact of bubble dissolution on the dissolved methane concentration, and (c) the distribution and activity of anaerobic microbial communities in the water column that may utilize the bubble-transported methane [41]. During the multiple crossings of VMV between 9 and 12 June 2003 (Fig. 6C) we observed that the flare significantly changed its shape above 1200 mwd, becoming much narrower (Fig. 7C). With a 1300-m flare height and a release depth of 2068 mwd the flare at VMV is certainly amongst the deepest and to our knowledge the highest reported flare so far.

During return surveys in June 2003, we obtained an even better spatial coverage of the NSS (Fig. 6D) and

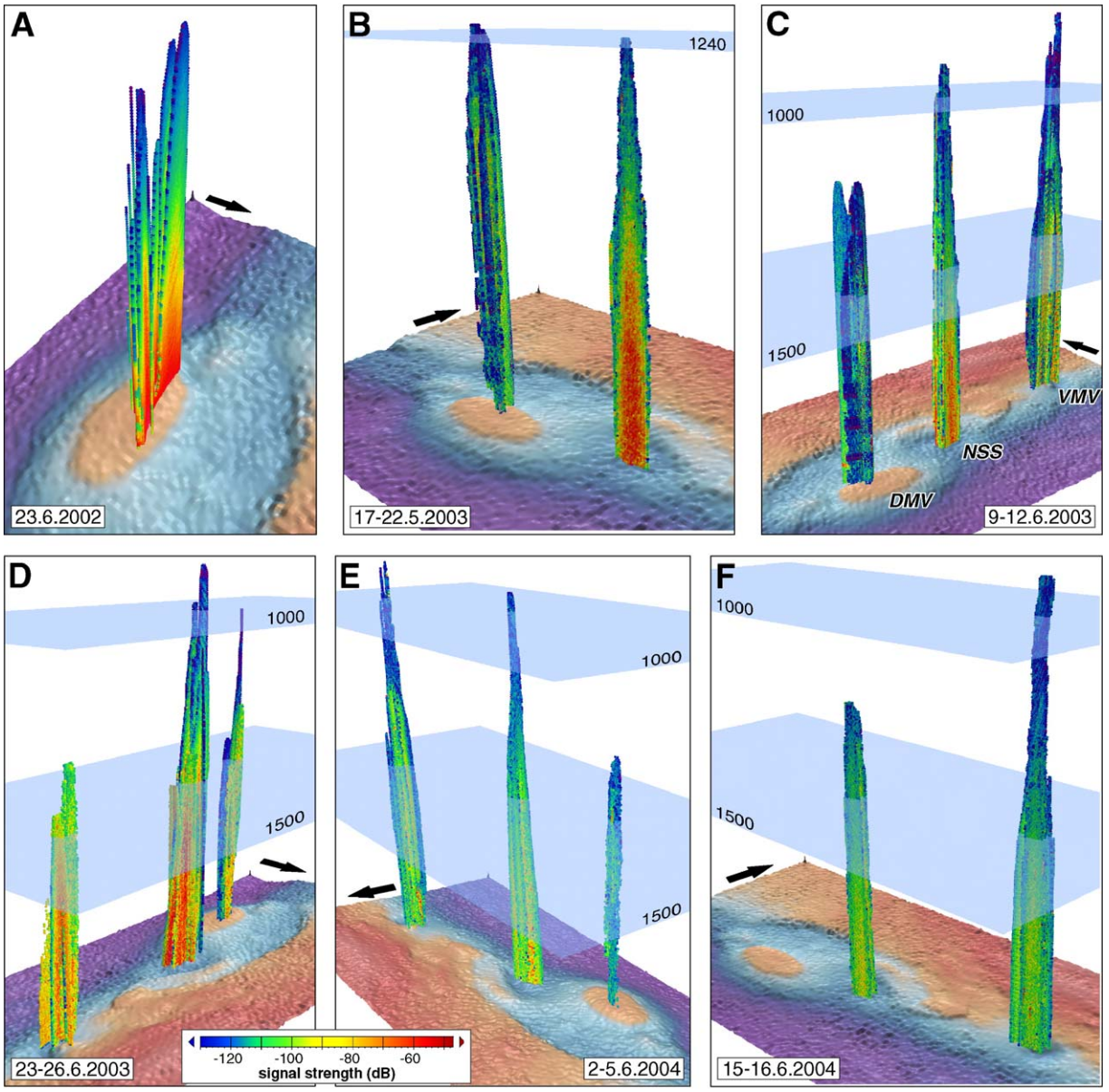

Fig. 7. (A) 3D view from 54° showing the registered flares on the 23 June 2002. Well visible are the different heights of the western flare (background) which becomes higher from south to north. Less obvious from this direction is that the N–S trending line of the eastern flare (foreground) shows the same height as the NE–SW trending lines. (B) View from 123° showing the much stronger backscatter signals at NSS and an 837-m-high flare at DMV. The blue plain is at 1240 m water depth. (C) View from 223° showing the flares above all three bubble locations. DMV shows only very weak backscatter values and a low spatial distribution. NSS and VMV have similar backscattering strength but the rising height at VMV is 150 m higher. Blue plains are in 1500 and 1000 m water depth. (D) View from 52° showing a strong but less high flare above VMV at the left and a very strong and high flare above NSS. The flare at DMV extends it height with respect to the previous observations, but becomes very thin above 1410 m water depth. (E) View from 329 showing the very high flare above NSS and VMV as well as the almost vanished flare above DVM with a rather thin root. (F) View from 127° with a very high flare above VMV and a significantly lower flare above NSS. The black arrows point towards north.

monitored the flares of the other two sites by four parallel lines crossing all sites within 4 h on 23 June 2003. Based on these almost simultaneous observations, we can conclude that all sites (DMV, NSS and VMV) were continuously active at the same time on 23 June 2003. The larger flare height (i.e. 1220 m) at NSS with respect to DMV and VMV might be artificial due to less survey time and lower line density at these two sites

(Fig. 7D). Despite their much lower flare height, their backscatter signals are of similar strength as at NSS which did not exceed −70 dB level.

The four NE–SW running parallel lines of 23 June 2003 were repeated twice in June 2004. On 2 June 2004, the flare at DMV had both a much lower height and intensity than during previous years. Only 13 days later, on 15 June 2004, it had completely disappeared (Figs. 6E, F and 7E, F). Also the flares above NSS and VMV decreased in height and backscatter intensity during June 2004. The steadily decreasing intensity and finally the complete disappearance of the flare at DMV in June 2004 and the concurrent decrease at NSS and VMV indicates a general decline in the fluid-venting activity in this area from 2003 to 2004, from SW towards NE. Subsequent surveys in August 2004 confirmed that no bubbles were released at DMV, but that NSS and VMV remained active (E. F. Shnyukov, personal communication).

4.2. Are the flares really caused by bubbles?

Hydroacoustics is very sensitive in detecting even small bubbles in the water column, which are hard or even impossible to observe visually. The ultimate confirmation that bubbles are indeed the cause of the observed backscatter signals would of course be provided by direct observations at the seep site itself. However, the required equipment has to be available and the typically very small-scale bubble-releasing spots have to be found. Despite these uncertainties, flares are nevertheless most often attributed to bubbles, although other explanations such as rising gas-hydrate particles, oil droplets, sediment particles or less dense water bodies are given as well [1,7,20].

With respect to our observations of acoustic flares above the mud volcanoes in the Sorokin Trough, we are confident that the backscattering in the water column at all three flare sites is indeed caused by bubbles, because:

(a) echogram patterns and particular linear features similar to those observed have been confirmed by in situ experiments to be caused by bubbles [22]
(b) the received signal strength and observed rising speeds fit perfectly with those of bubbles
(c) the backscattering from fish as described by Ostrovsky [3] can be excluded due to the anoxic conditions at those water depths in the Black Sea
(d) strong density changes in the water column due to thermal/saline plumes are not present in the area

The two features referred to as (a) and (b) are evident in our echograms and prove the occurrence of bubbles by: (a) 'rising' strong backscatter signals which plot along a line that can be used to measure the rise velocity; and (b) backscatter values that are in the range of what would be produced by gas bubbles in that particular water depth and acoustic frequency. Fig. 8 shows an echogram from DMV on which rising bubbles are clearly seen. Measuring the rise velocity of bubble lines near the seafloor and at the top of the flare results in values of 19–22 and 12–14 cm/s, respectively. These rise velocities are in the typical range for 'dirty' rising bubbles, which varies between 10 and 28 cm/s for

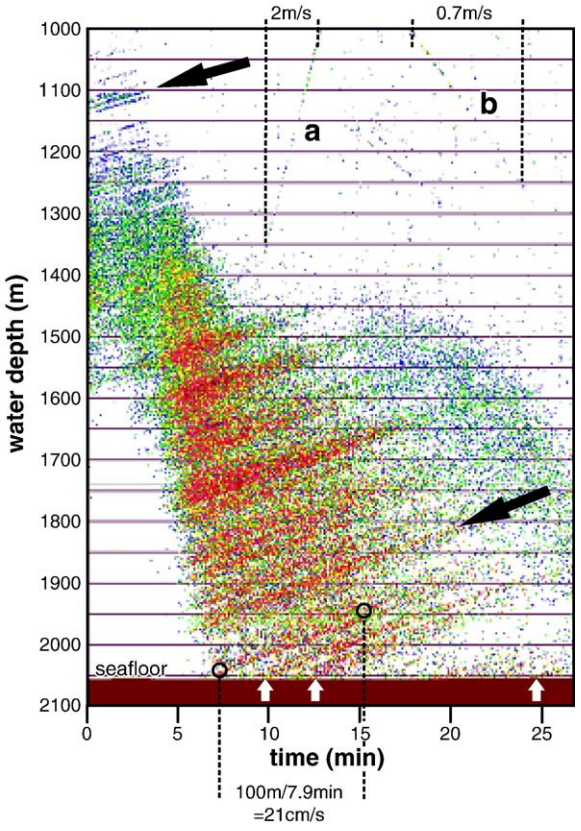

Fig. 8. Typical echogram showing the flare-shaped hydroacoustic backscatter signals on top of DMV. During the 27 min of observation the ship drifted within an area of about 200 m. Lines in echograms, as marked by black arrows, represent the rising of denser bubble clouds. The time axis corresponds to pings with a ping rate of 4.5 s. Picking the time difference at two distinct depths (open black circles) at such a 'bubble-line' the bubble rising speed can be directly measured. The slight bending of bubble-lines indicate changing (decreasing) rising speeds due to bubble shrinkage. White arrows mark bubble release events which indicate that bubbles are not constantly released on short time scales. The two lines marked a and b are reflections from an upward (a, 2 m/s) and downward (b, 0.7 m/s) going CTD.

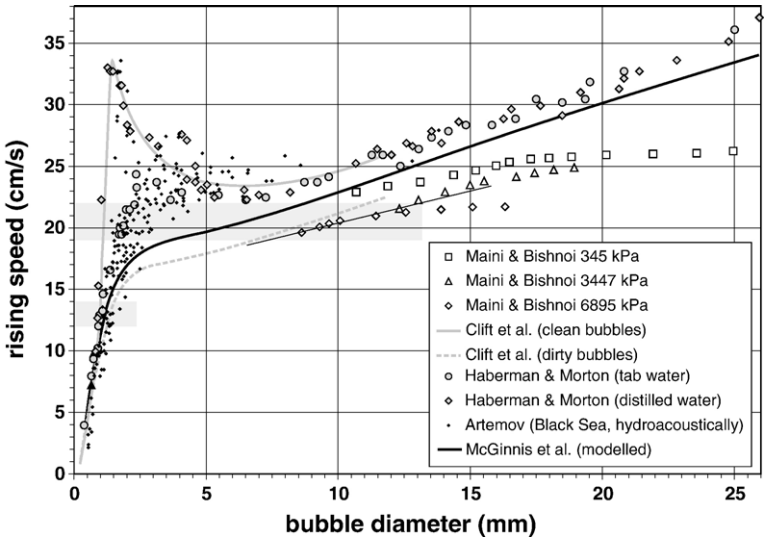

Fig. 9. Compiled data of rising speed versus bubble size. The typical relation for clean bubbles in distilled water as documented from Haberman and Morton [53] and modeled in Clift et al. [54] is not valid for the natural environment where surfactants decrease the rise velocity. Important here are data presented by Maini and Bishnoi [55] which give rise velocities between 19 and 22 cm/s for gas hydrate rimmed bubbles between 8.5 and 13 mm diameter.

bubbles between 1 and 15 mm in diameter, respectively (Fig. 9; and summary in McGinnis et al. [49]. Unfortunately, the rather simple correlation between bubble size and rise velocity of 'clean' bubbles in tap or distilled water [53,54] cannot be directly applied in natural environments where surfactants (sediment particles, organic matter, and oil) or a skin of gas hydrate decrease the rising speed sometimes drastically [7,53,55–57]. The echogram example of Fig. 8 shows slower rising velocities at the top of the flare, which mirrors the presence of bubbles that are smaller than those released from the seafloor.

4.3. Modeling the bubble rising height

Observing bubbles that rise over 1300 m through the water column brings up the question how bubbles can exist over such a long time (108 min, with a rising speed of 20 cm/s) without being dissolved. One possible explanation could be the formation of a gas-hydrate skin as already proposed – and observed – by several authors [50,58,59]. Such a skin would form almost immediately around the bubble upon its release from the sediment within the GHSZ, or perhaps already in the sediment, and would drastically decreases the gas exchange between the bubble and the surrounding sea water.

McGinnis et al. [49] utilize this gas-hydrate skin concept to model the evolution of bubble sizes and gas composition in 1300-m-high rising bubbles in the DMV area assuming that pure methane bubbles were released at the seafloor. The physical and chemical boundary conditions of the water column correspond to those shown in Fig. 3. As stated by McGinnis et al. [49], the gas concentrations in the water, i.e. changes in H_2S and CO_2, can be neglected in the model calculations due to the extreme depth. As both gasses are highly soluble, the local dissolved concentrations are far below saturation.

Using the methane–bubble dissolution data obtained by Rehder et al. [50], McGinnis et al. [49] calibrated their bubble-rise model to predict the bubble behavior within the GHSZ. They argue that for the experiments of Rehder et al. [50] the much shallower depth of around 800 m is responsible for a later 'freezing' of the bubble at around 3.5 mm bubble diameter as marked by the significant change in the shrinking rate in the data from Rehder et al. [50]. Assuming that the mass-transfer coefficient of bubbles completely coated with a gas-hydrate skin ('frozen bubbles') is the same in 2000 and 800 mwd, the model predicts that bubbles immediately coated by gas hydrate when released from the seafloor only have to be 9 mm in diameter to rise 1300 m through the water column (Fig. 10). Only within the last 50 m the bubbles shrinks below 1 mm, which is still in agreement with the hydroacoustically observed rising speeds. Only slightly larger bubbles (11.8 mm) would be needed to reach the top of the flare as 5.5 mm sized bubbles and to become dissolved only at the sea surface, if the slower hydrate-skin-induced mass transfer would apply the

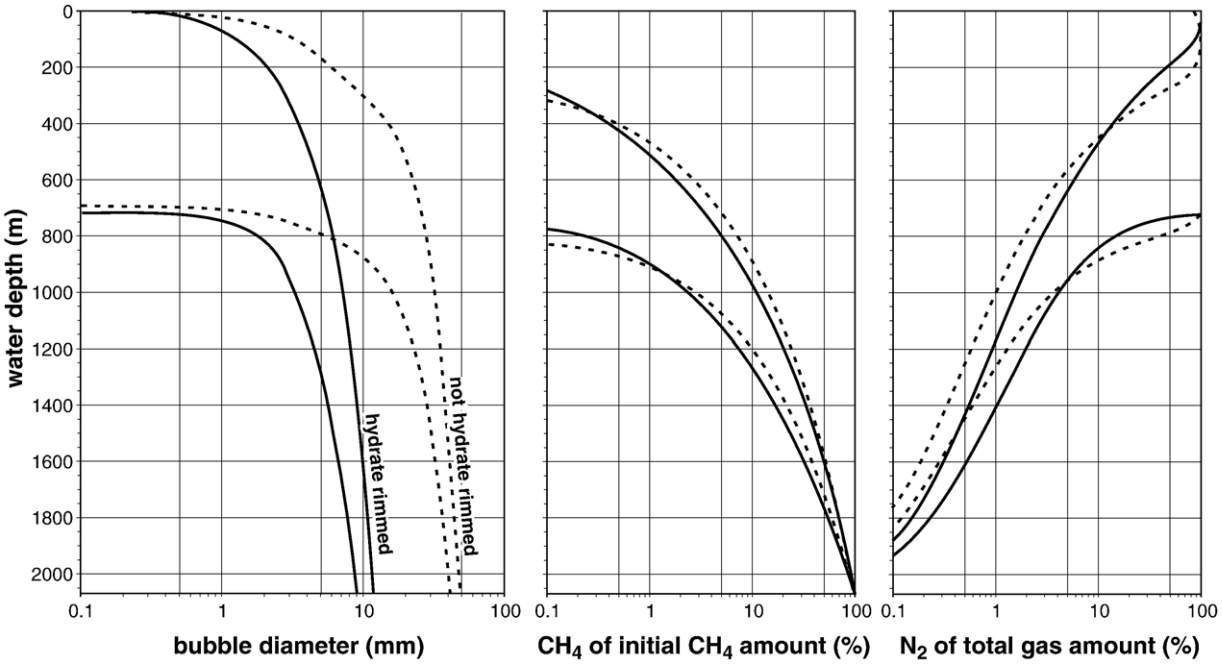

Fig. 10. Model results of four different gas bubbles, two of which having no gas hydrate rim (dashed lines) and two forming an instantaneous gas hydrate rim that drastically decrease the mass transfer coefficient (solid lines). To reach the detected flare high of about 1300 m, a bubble of 'only' 9 mm in diameter is needed. This size is very reasonable; the mass transfer of gas hydrate rimmed bubbles is calibrated by McGinnis et al. [49] using experiments by Rehder et al. [50]. With respect to not-rimmed bubbles, this mass transfer is almost ten times decreased.

entire way through the water column. That fact that bubbles do keep the slower mass transfer for quite a while after leaving the GHSZ is shown by the data of Rehder et al. [50] and is discussed by McGinnis et al. [49]. However, it seems rather unlikely that the gas-hydrate coating will remain intact during a 700-m-high rise and thus model results for the 11.8 mm frozen bubble are certainly not correct above the gas-hydrate phase boundary at 695 mwd.

According to the experimental bubble-rise data from Maini and Bishnoi [55], the modeled bubble size of 9 mm fits very well with the rising-speed range of 19–22 cm/s as measured close to the seafloor (Fig. 9). This coincidence, the very reasonable initial bubble size and the knowledge that gas-hydrate skins form rapidly around bubbles [58,59] strongly supports the hypothesis that the formation of gas-hydrate coatings allows methane bubbles released at mud volcanoes at 2000 mwd to rise through the water column for over 1300 m without being dissolved, and that they are detectable during hydroacoustic surveys.

5. Summary and conclusions

As part of four Black Sea cruises, hydroacoustic surveys were undertaken between January 2002 and June 2004, during which hydroacoustic plumes – flares – were detected above three mud volcanoes in about 2080 m water depth in the Sorokin Trough. With 1300 m height, these flares are the highest and with 2080 m water depth they are among the deepest flares reported so far. The hydroacoustic investigations show rising speeds of the hydroacoustic backscatterers varying between 19 and 22 cm/s close to the seafloor and between 12 and 14 cm/s at the top of the flare. As the Black Sea is anoxic below ~120 m, no fish or other organisms can be responsible for the backscattering. Therefore, methane bubbles released from the mud volcanoes are the most likely cause of these high flares. In the course of our hydroacoustic surveys, we observed that DMV was not active in January 2002, but found a very high flare in June 2002, May–June 2003 and May 2004. This high flare vanished in June 2004 and DMV remained inactive in August 2004. The two other mud volcanoes (NSS and VMV) were active whenever surveyed, but also showed a slight decrease in activity, as indicated by lower flare heights and by less intense backscattering, during our last observations in 2004. When active, all three mud volcanoes released bubbles at the same time and we are confident that they did so constantly, also in between our surveys. The mechanisms for the

methane oversaturation are either the pressure decrease of deeply derived, strongly methane-enriched fluids and/or the thermal decomposition of gas hydrates due to the upward migration of warmer fluids. As fluid migration and heat transport in sediments are rather slow processes, rapid changes in bubble releasing activity are unlikely. It is unclear if this episode represents a violent gas eruption comparable to those observed on land i.e. in Azerbaijan (Lokbatan mud volcano that at least erupted 23 times since 1829; [60]) or if we witnessed 'only' a period of slightly increased activity that was just intense enough to be detected by hydroacoustic. However, our observations give a first example of the lifetime and of the variations in activity of a single episode of bubble-release from an underwater mud volcano.

With 1300 m rising height the observed flares are the highest reported so far. Observing bubbles that rise over 1300 m through the water column brings up the question how bubbles can exist over such a long distance. We propose, supported by modeling the bubble dissolution using the recently presented model by McGinnis et al. [49], that this is due to the formation of a gas-hydrate coating on the bubbles. As suggested by Rehder et al. [50] and observed by Brewer et al. [59], bubbles within the GHSZ immediately form a gas-hydrate skin that decreases the mass transfer between the bubble and the surrounding water by approximately ten times. The model predicts that a bubble with an initial diameter of 9 mm upon release at the seafloor would survive a 1300-m-high rise through the water column, if protected by a gas-hydrate coating. The measured rising speed of 19–22 cm/s is completely in agreement with the rising speed of gas-hydrate-rimmed bubbles of this size [55] which are in the typical size range of bubbles released at seep sites.

Acknowledgement

Our thanks go to the crew of *RV Professor Vodyanitskiy* for their great enthusiasm, help and hospitality during the cruises. Also thanks to all CRIMEA project members and particularly to Stanley Beaubien (University of Roma "La Sapienza") for supporting us with gas analyses. Finally we have to express our thanks to the EU by financing our work through grant EVK-2-CT-2002-00162. Financial support was also given through the R&D-Programme GEOTECHNOLOGIEN funded by the German BMBF and DFG (Grant No. 03G0600D). This is publication GEOTECH–206.

References

[1] C.K. Paull, W. Ussler III, W.S. Borowski, F.N. Spiess, Methane-rich plumes on the Carolina continental rise: associated with gas hydrates, Geology 23 (1995) 89–92.
[2] W.S. Borowski, C.K. Paull, W. Ussler III, Carbon cycling within the upper methanogenic zone of continental rise sediments: an example from the methane-rich sediments overlying the Blake Ridge gas hydrate deposits, Mar. Chem. 57 (1997) 299–311.
[3] P. Van Rensbergen, M. De Batist, J. Klerkx, R. Hus, J. Poort, M. Vanneste, N. Granin, O. Khlystov, P. Krinitsky, Sublacustrine mud volcanoes and methane seeps caused by dissociation of gas hydrates in Lake Baikal, Geology 30 (2002) 631–634.
[4] M.E. Torres, J. McManus, D.E. Hammond, M.A. de Angelis, K. U. Heeschen, S.L. Colbert, M.D. Tryon, K.M. Brown, E. Suess, Fluid and chemical fluxes in and out of sediments hosting methane hydrate deposits on Hydrate Ridge, OR: I. Hydrological provinces, Earth Planet. Sci. Lett. 201 (2002) 525–540.
[5] M. De Batist, J. Klerkx, P. Van Rensbergen, M. Vanneste, J. Poort, A.Y. Golmshtok, A.K. Kremlev, O.M. Khlystov, P. Krinitsky, Active hydrate destabilization in Lake Baikal, Siberia? Terra Nova 14 (2002) 436–442.
[6] I. Ostrovsky, Methane bubbles in Lake Kinneret: quantification and temporal and spatial heterogeneity, Limnol. Oceanogr. 48 (2003) 1030–1036.
[7] I. Leifer, I.R. MacDonald, Dynamics of the gas flux from shallow gas hydrate deposits: interaction between oily hydrate bubbles and the oceanic environment, Earth Planet. Sci. Lett. 210 (2003) 411–424.
[8] J. Greinert, G. Bohrmann, E. Suess, Gas hydrate-associated carbonates and methane-venting at Hydrate Ridge: classification, distribution, and origin of authigenic lithologies, in: C.K. Paull, P.W. Dillon (Eds.), Natural Gas Hydrates: Occurrence, Distribution, and Dynamics, Geophys. Monogr., vol. 124, 2001, pp. 99–113.
[9] B.M.A. Teichert, A. Eisenhauer, G. Bohtmann, A. Haase-Schramm, B. Bock, P. Linke, U/Th systematics and ages of authigenic carbonates from Hydrate Ridge, Cascadia Margin: recorders of fluid flow variations, Geochim. Cosmochim. Acta 67 (2003). doi:10.1016/S0016-7037(03)00128-5.
[10] C.K. Paull, B. Schlining, W. Ussler III, J.B. Paduan, D. Caress, H.G. Greene, Distribution of chemosynthetic biological communities in Monterey Bay, California, Geology 33 (2005) 85–88.
[11] M.V. Ivanov, G.G. Polikarpov, V.F. A.Yu. Lein, V.N. Galtchenko, S.B. Egorov, M.B. Gulin, I.I. Gulin, Yu.M. Miller, V.I. Kuptsov, Biogeochemistry of the carbon cycle in the region of methane gas seeps of the Black Sea, Dokl. AN USSR 320 (5) (1991) 1235–1240 (in Russian).
[12] A. Boetius, K. Ravenschlag, C.J. Schubert, D. Rickert, F. Widdel, A. Gieskes, R. Amann, B.B. Joergensen, U. Witte, O. Pfannkuche, A microbial consortium apparently mediating anaerobic oxidation of methane, Nature 407 (2000) 623–626.
[13] W. Michaelis, R. Seifert, K. Nauhaus, T. Treude, V. Thiel, M. Blumenberg, K. Knittel, A. Gieseke, K. Peterknecht, T. Pape, A. Boetius, R. Amann, B.B. Jorgensen, F. Widdel, J. Peckmann, N. V. Pimenov, M.B. Gulin, Microbial reefs in the Black Sea fueled by anaerobic oxidation of methane, Science 297 (2002) 1013–1015.
[14] K. Nauhaus, A. Boetius, M. Krüger, F. Widdel, In vitro demonstration of anaerobic oxidation of methane coupled to sulphate reduction in sediment from a marine gas hydrate area, Environ. Microbiol. 4 (2002) 296–305.

[15] T. Treude, A. Boetius, K. Knittel, K. Wallmann, B.B. Jørgensen, Anaerobic oxidation of methane above gas hydrates at Hydrate Ridge, NE Pacific Ocean, Mar. Ecol., Prog. Ser. 264 (2003) 1–14.
[16] S. Sommer, O. Pfannkuche, P. Linke, R. Luff, J. Greinert, M. Drews, S. Gubsch, M. Pieper, M. Poser, T. Viergutz, The efficiency of the benthic filter – biological control of the emission of dissolved methane from sediments hosting shallow gas hydrates at Hydrate Ridge: 2. Glob. Biogeochem. Cycles. in press.
[17] M.T. Medigan, J. Martinko, J. Parker, Brock Biology of Microorganisms, Prentice-Hall, New Jersey, 2002. 1385 pp.
[18] K.U. Heeschen, W.C. Collier, M.A. de Angelis, E. Suess, G. Rehder, P. Linke, P. Klinkhammer, Methane sources, distributions, and fluxes from cold vent sites at Hydrate Ridge, Cascadia Margin, Glob. Biogeochem. Cycles 19 (2005), doi:10.1029/2004GB002266.
[19] U. Berner, J. Poggenburg, E. Faber, D. Quadfasel, A. Frische, Methane in ocean waters of the Bay of Bengal: its sources and exchange with the atmosphere, Deep-Sea Res. II 50 (2003) 925–950.
[20] R. Merewether, M.S. Olsson, P. Lonsdale, Acoustically detected hydrocarbon plumes rising from 2-km depths in the Guayamas Basin, Gulf of California, J. Geophys. Res. 90 (1985) 3075–3085.
[21] G.G. Polikarpov, V.N. Egorov, Evidence of the gas bubble streams from the Black Sea bottom, Visnik AN, UkrSSR 10 (1989) 108 (in Ukrainian).
[22] G.G. Polikarpov, V.N. Egorov, A.l. Nezhdanov, S.B. Gulin, Yu. D. Kulev, M.B. Gulin, The phenomenon of active gas escapes from mounts on the slope of the western Black Sea, Dokl. AN UkrSSR 12-B (1989) 13–16 (in Russian).
[23] L. Dimitrov, V. Dontcheva, Seabed pockmarks in the southern Bulgarian Black Sea zone, Bull. Geol. Soc. Den. 41 (1994) 24–33.
[24] P.R. Dando, P. Jensen, S.C.M. O'Hara, S.J. Niven, R. Schmaljohan, U. Schuster, L.J. Taylor, The effects of methane seepage at an intertidal/shallow subtidal site on the shore of the Kattegat, Vendsyssel, Denmark, Bull. Geol. Soc. Den. 41 (1994) 65–79.
[25] S. Zimmermann, R.G. Hughes, H.J. Flügel, The effect of methane seepage on the spatial distribution of oxygen and dissolved sulphide within a muddy sediment, Mar. Geol. 137 (1997) 149–157.
[26] T.F. Wever, F. Abegg, H.M. Fiedler, G. Fechner, I.H. Stender, Shallow gas in the muddy sediments of Eckernförde Bay, Germany, Cont. Shelf Res. 18 (1998) 1715–1739.
[27] E. Suess, M.E. Torres, G. Bohrmann, R.W. Collier, D. Rickert, C. Goldfinger, P. Linke, A. Hauser, H. Sahling, K. Heeschen, C. Jung, K. Nakamura, J. Greiner, O. Pfannkuche, A. Trehu, G. Klinkhammer, M.J. Whiticar, A. Eisenhauer, B. Teichert, M. Elvert, Seafloor methane hydrates at Hydrate Ridge, Cascadia Margin, in: C.K. Paull, W.P. Dillon (Eds.), Natural Gas Hydrates: Occurrence, Distribution, and Detection. Geophysical Monograph, vol. 124, 2001, pp. 87–98.
[28] J.S. Hornafius, D. Quigley, B.P. Luyendyk, The world's most spectacular marine hydrocarbon seeps (Coal Oil Point, Santa Barbara Channel, California): quantification of emission, J. Geophys. Res. 104 (1999) 20703–20711.
[29] K.U. Heeschen, A.M. Trehu, R.W. Collier, E. Suess, G. Rehder, Distribution and height of methane bubble plumes on the Cascadia Margin characterized by acoustic imaging, Geophys. Res. Lett. 30 (2003), doi:10.1029/2003GL016974.
[30] B. Flemming (Ed.), Geo-Marine Letters, vol. 23 Number 3–4, Springer-Verlag, Berlin, 2003. 221 pp.
[31] Y.G. Artemov, Software support for investigation of natural methane seeps by hydroacoustic method, Mar. Ecol. J. 5 (2006) 57–71.
[32] I. Leifer, I., A. Judd, Oceanic methane layers: the hydrocarbon seep bubble deposition hypothesis, Terra Nova 14 (2002) 417–424.
[33] G. Bohrmann, M. Ivanov, J.-P. Foucher, V. Spiess, J. Bialas, J. Greinert, W. Weinrebe, F. Abegg, G. Aloisi, Y. Artemov, V. Blinova, M. Drews, F. Heidersdorf, A. Krabbenhöft, I. Klaucke, S. Krastel, T. Leder, I. Polikarpov, M. Saburova, O. Schmale, R. Seifert, A. Volkonskaya, M. Zillmer, Mud volcanoes and gas hydrates in the Black Sea: new data from Dvurechenskii and Odessa mud volcanoes, Geo Mar. Lett. 23 (2003) 239–249.
[34] S. Krastel, S. Spiess, W. Weinrebe, B. Bohrmann, P. Shashkin, F. Heidersdorf, Acoustic investigations of mud volcanoes in the Sorokin Trough, Black Sea, Geo Mar. Lett. 23 (2003) 230–238.
[35] G. Aloisi, M. Drews, K. Wallmann, G. Bohrmann, Fluid expulsion from the Dvurechenskii mud volcano (Black Sea): part I. Fluid sources and relevance to Li, B, Sr, I and dissolved inorganic nitrogen cycles, Earth Planet. Sci. Lett. 225 (2004) 347–363.
[36] V.N. Blinova, M.K. Ivanov, G. Bohrmann, Hydrocarbon gases in deposits from mud volcanoes in the Sorokin Trough, northeastern Black Sea, Geo Mar. Lett. 23 (2003) 250–257.
[37] A. Stadnitskaia, T.G. Muyzera, B. Abbasa, M.J.L. Coolena, N.C. Hopmansa, M. Baasa, T.C.E. van Weeringa, M.K. Ivanov, E. Poludetkina, J.S. Sinninghe Damste, Biomarker and 16S rDNA evidence for anaerobic oxidation of methane and related carbonate precipitation in deep-sea mud volcanoes of the Sorokin Trough, Black Sea, Mar. Geol. 217 (2005) 67–96.
[38] W.S. Reeburgh, B.B. Ward, S.C. Whalen, K.A. Sandbeck, K.A. Kilpatrick, L.J. and, Black Sea methane geochemistry, Deep-Sea Res. 38 (1991) 1189–1210.
[39] C. Saydam, S. Tugrul, O. Basturk, T. Oguz, Identification of the oxic/anoxic interface by isopycnal surfaces in the Black Sea, Deep-Sea Res., Part 1, Oceanogr. Res. Pap. 40 (7) (1993) 1405–1412.
[40] T. Oguz, Role of physical processes controlling oxycline and suboxic layer structures in the Black Sea, Glob. Biogeochem. Cycles 16 (2002), doi:10.1029/2001GB001465.
[41] C.J. Schubert, E. Durisch-Kaiser, C.P. Holzner, L. Klauser, B. Wehrli, O. Schmale, J. Greinert, D.F. McGinnis, M. De Batist, R. Kipfer, Methanotrophic microbial communities associated with bubble plumes above gas seeps in the Black Sea, Geochem. Geophys. Geosyst. 7 (2006), doi:10.1029/2005GC001049.
[42] E.V. Stanev, E.L. Peneva, Regional sea level response to global climatic changes: Black Sea examples, Glob. Planet. Change 32 (2002) 33–47.
[43] L. Anon, Simrad EK500 Scientific Echo Sounder Instruction Manual. Simrad Subsea, P2172E (1991).
[44] G. Bohrmann, S. Schenck, RV Meteor Cruise Report M52/1, MARGASCH, Marine gas hydrates in the Black Sea, GEOMAR-Rep. 108 (2002) (202 pp.).
[45] S. Lammers, E. Suess, An improved head-space analysis method for methane in seawater, Mar. Chem. 47 (1994) 115–125.
[46] G. Rehder, R.S. Keir, E. Suess, M. Rhein, Methane in the northern Atlantic controlled by microbial oxidation and atmospheric history, Geophys. Res. Lett. 26 (1999) 587–590.
[47] E.D. Sloan, Clathrate Hydrates of Natural Gases, Marcel Dekker, Inc., New York, 1998. 641 pp.

[48] G.R. Dickens, M.S. Quinby-Hunt, Methane hydrate stability in seawater, Geophys. Res. Lett. 21 (1994) 2115–2118.
[49] D.F. McGinnis, J. Greinert, Y. Artemov, S.E. Beaubien, and A. Wüest, The fate of rising methane bubbles in stratified waters: what fraction reaches the atmosphere? J. Geophys. Res. (in press).
[50] G. Rehder, P.W. Brewer, E.T. Peltzer, G. Friederich, Enhanced lifetime of methane bubble streams within the deep ocean, Geophys. Res. Lett. 29 (2002) 21–24.
[51] E.F. Shnyukov, A.A. Pasynkov, S.A. Kleshenko, V.A. Kutniy, The largest gas fountain of the Black Sea Basin, Geophys. J. 25 (2003) 170–176 (in Russian).
[52] E.F. Shnyukov, A.Y. Lein, V.N. Egorov, S.A. Kleshenko, S.B. Gulin, Y.G. Artemov, H.A. Arslanov, V.A. Kutniy, Discovery of biogenic carbonate chimneys at abyssal depths in the Black Sea, Rep. Natl. Acad. Sci. Ukr. 1 (2004) 118–122 (in Russian).
[53] W.L. Haberman, R.K. Morton, An experimental study of bubbles moving in liquids, Proc. Am. Soc. Civ. Eng. 80 (1954) 379–427.
[54] R. Clift, J.R. Grace, M.E. Weber, Bubbles, Drops, and Particles, Academic Press, New York, 1978, p. 380.
[55] B.B. Maini, P.R. Bishnoi, Experimental investigation of hydrate formation behaviour of a natural gas bubble in a simulated deep sea environment, Chem. Eng. Sci. 36 (1981) 183–189.
[56] S.S. Ponoth, J.B. McLaughlin, Numerical simulation of mass transfer for bubbles in water, Chem. Eng. Sci. 55 (2000) 1237–1255.
[57] I. Leifer, K. Patro, The bubble mechanism for methane transport from the shallow sea bed to the surface: a review and sensitivity study, Cont. Shelf Res. 22 (2002) 2409–2428.
[58] N.A. Gumerov, G.L. Chahine, Dynamics of bubbles in conditions of gas hydrate formation, 8th International Offshore and Polar Engineering Conference, Montreal, Canada, 1998.
[59] P.G. Brewer, C. Paull, E.T. Peltzer, W. Ussler, G. Rehder, G. Friederich, Measurements of the fate of gas hydrates during transit through the ocean water column, Geophys. Res. Lett. 29 (2002), doi:10.1029/2002GL014727.
[60] G. Etiope, A. Feyzullayev, C.L. Baciu, A.V. Milkov, Methane emissions from mud volcanoes in eastern Azerbaijan, Geology 32 (2004) 465–468.
[61] V.N. Egorov, G.G. Polikarpov, S.B. Gulin, Y.G. Artemov, N.A. Stokozov, S.K. Kostova, Modern conception about forming-casting and ecological role of methane gas seeps from bottom of the Black Sea, Mar. Ecol. J. 2 (2003) 5–26.